STEEL-FREE CONCRETE BRIDGE DECKS

Final Report
December 2024

Principal Investigators:

Eric Landis and William Davids

Authors:

Arnav Acharya, Erfan Najaf, William Davids, and Eric Landis

Sponsored By

Transportation Infrastructure Durability Center

List other Sponsors if applicable (i.e. MaineDOT)

TIDC

Transportation Infrastructure Durability Center

AT THE UNIVERSITY OF MAINE

A report from

University of Maine

Department Civil & Environmental Engineering

5711 Boardman Hall

Orono, ME 04469

Phone: 207 581-2173

Website

THE UNIVERSITY OF MAINE · UMASS LOWELL · WESTERN NEW ENGLAND UNIVERSITY WNE · UCONN · THE UNIVERSITY OF RHODE ISLAND · The UNIVERSITY of VERMONT

About the Transportation Infrastructure Durability Center

The Transportation Infrastructure Durability Center (TIDC) is the 2018 US DOT Region 1 (New England) University Transportation Center (UTC) located at the University of Maine Advanced Structures and Composites Center. TIDC's research focuses on efforts to improve the durability and extend the life of transportation infrastructure in New England and beyond through an integrated collaboration of universities, state DOTs, and industry. The TIDC is comprised of six New England universities, the University of Maine (lead), the University of Connecticut, the University of Massachusetts Lowell, the University of Rhode Island, the University of Vermont, and Western New England University.

U.S. Department of Transportation (US DOT) Disclaimer

Acknowledgements

Funding for this research is provided by the Transportation Infrastructure Durability Center at the University of Maine under grant 69A3551847101 from the U.S. Department of Transportation's University Transportation Centers Program. [Include any acknowledgements for other contributors (i.e. your university or contributing DOTs/industry partners) here.]

1. Report No.	2. Government Accession No.	3. Recipient Catalog No.
4 Title and Subtitle Steel-Free Concrete Bridge Decks		5 Report Date 6 Performing Organization Code
7. Author(s) Arnav Acharya, Erfan Najaf, William Davids, and Eric Landis		8 Performing Organization Report No.
9 Performing Organization Name and Address		10 Work Unit No. (TRAIS) 11 Contract or Grant No.
12 Sponsoring Agency Name and Address		13 Type of Report and Period Covered 14 Sponsoring Agency Code
15 Supplementary Notes		

16 Abstract

This report investigates the development and structural performance of steel-free concrete bridge decks as a solution to reinforcement corrosion in cold-climate infrastructure. The study evaluates the integration of Basalt Fiber-Reinforced Concrete (BFRC) and Glass Fiber-Reinforced Polymer (GFRP) rebars through a two-phase experimental approach. Phase I focuses on mix design optimization, analyzing the effects of basalt fiber volumetric fractions (0% to 1.2%) on workability and mechanical properties. Results indicate that while a 1.0% fiber content increases flexural capacity by 40% and reduces shrinkage by up to 21%, a threshold of 0.5% is critical for maintaining field-appropriate workability. Phase II examines the synergy between the optimized BFRC mix and GFRP rebars. Four-point bending tests demonstrate that adding GFRP reinforcement to BFRC increases flexural strength by up to 272% compared to unreinforced specimens. Furthermore, the inclusion of fibers effectively mitigates the brittle failure typically associated with GFRP, enhancing post-cracking ductility and crack distribution. The findings suggest that a hybrid BFRC-GFRP system provides a durable, high-performance, and corrosion-resistant alternative to traditional steel-reinforced concrete for bridge deck applications.

17 Key Words	18 Distribution Statement
Basalt Fiber-Reinforced Concrete (BFRC), Glass Fiber-Reinforced Polymer GFRP), Basalt Minibars, Structural Durability, Shrinkage	No restrictions. This document is available to the public through

19 Security Classification (of this report)	20 Security Classification (of this page)	21 No. of pages	22 Price
Unclassified	Unclassified		

Technical Report Documentation Page

Form DOT F 1700.7 (8-72)

Contents

List of Figures

List of Tables

Chapter 1:Introduction and Background

The United States relies on a vast network of bridges to maintain economic stability and transportation efficiency. Most of these structures utilize concrete bridge decks due to their ability to withstand heavy loads and harsh environmental conditions. However, the longevity of these structures is significantly compromised by the degradation of their internal components, primarily the steel reinforcement.

1-1- Project Motivation

The primary motivation for this project is the **economic and structural crisis caused by the corrosion of steel reinforcement**. In cold climates, such as the Northeast United States, the frequent use of de-icing salts (magnesium chloride, calcium chloride, and sodium chloride) introduces chloride ions into the concrete. These ions penetrate the porous concrete matrix, reaching the steel rebar and destroying its protective passive layer.

The resulting corrosion leads to:

- **Structural Damage:** Rust occupies a larger volume than the original steel, creating internal expansive pressure that causes concrete cracking, spalling, and delamination.
- **High Maintenance Costs:** As of the early 21st century, the annual direct cost of corrosion for highway bridges in the U.S. was estimated at approximately **$10 billion**.
- **Safety Risks:** Deteriorating bridge decks reduce the safe load-carrying capacity of the infrastructure and necessitate frequent, disruptive repairs.

Traditional mitigation strategies, such as cathodic protection or epoxy coatings, have provided only temporary relief. Therefore, there is an urgent need for a **"Steel-Free" bridge deck system**. By replacing corrosion-prone steel with **Glass Fiber-Reinforced Polymer (GFRP) rebars** and enhancing the concrete matrix with **Basalt Fibers**, this research aims to develop a system that is inherently immune to chloride-induced corrosion. This hybrid approach not only promises a longer service life for bridge infrastructure but also seeks to overcome the brittle failure mechanisms typically associated with FRP-reinforced structures.

1-2- Research, Objectives, and Tasks

The primary objective of this research is to develop and characterize a corrosion-resistant, "steel-free" concrete system that maintains structural integrity and ductility comparable to traditional reinforced concrete. To achieve this, the study investigates the synergy between a high-performance **Basalt Fiber-Reinforced Concrete (BFRC)** matrix and **Glass Fiber-Reinforced Polymer (GFRP)** internal reinforcement.

1.2.1 Research Objectives

The specific goals of this investigation are to:

1. **Optimize Mix Design:** Determine the ideal volumetric fraction of basalt fibers that enhances mechanical properties (flexural and compressive strength) without compromising the workability required for field placement.
2. **Mitigate Brittle Failure:** Leverage the crack-bridging capabilities of basalt fibers to improve the post-cracking behavior and ductility of GFRP-reinforced sections, which are inherently brittle.
3. **Evaluate Durability Factors:** Analyze the impact of fiber reinforcement on drying shrinkage to assess long-term volumetric stability.
4. **Validate Structural Performance:** Conduct large-scale testing to compare the load-deflection behavior of BFRC beams against traditional plain concrete sections reinforced with GFRP.

1.2.2 Research Tasks

To meet these objectives, the project was organized into the following systematic tasks:

- **Task 1: Material Characterization (Phase 1)**
  - Develop 11 unique mix designs using two aggregate sizes (3/4" and 3/8").
  - Vary basalt fiber content from 0% to 1.2% by volume.
  - Perform slump tests to quantify workability and determine the "homogeneity threshold."
  - Conduct three-point bending, compression, and 28-day shrinkage tests.
- **Task 2: Structural Beam Testing (Phase 2)**

- Design beam specimens using AASHTO LRFD specifications for GFRP-reinforced concrete.
- Manufacture 4" x 4" x 54" beams with varying rebar counts (1-bar vs. 2-bar systems) and optimized fiber content.
- Execute four-point bending tests using an Instron load frame to measure peak load, mid-span deflection, and toughness.

- **Task 3: Analysis and Modeling**
  - Compare Phase 1 and Phase 2 data to identify synergistic effects.
  - Perform moment-curvature analysis to predict the load-deflection behavior of the hybrid system.
  - Formulate recommendations for the application of BFRC in bridge deck construction.

1-3- Report Overview

This report is organized into five primary chapters that document the research progression from initial material development to full-scale structural testing of a steel-free bridge deck system. The structure of the report is as follows:

- **Chapter 1: Introduction and Background** establishes the motivation for the study, focusing on the $10 billion annual cost of bridge corrosion in the United States. It defines the research objectives, the specific tasks required to validate a non-corrosive alternative, and the scope of the two-phase experimental program.
- **Chapter 2: Literature Review** provides a comprehensive look at the durability crisis of reinforced concrete, focusing on chemical degradation like carbonation and chloride-induced corrosion. It further explores the material science of Fiber-Reinforced Polymer (FRP) and Fiber-Reinforced Concrete (FRC), establishing the theoretical synergy between basalt fibers and GFRP rebars.
- **Chapter 3: Methodology** details the experimental procedures for both Phase 1 (Material Optimization) and Phase 2 (Structural Testing). This chapter covers the

standardized mixing protocols adapted from MaineDOT, specimen fabrication techniques—including the heat-treatment process for bending GFRP rebars—and the configurations for the three-point and four-point bending tests.

- **Chapter 4: Results and Discussion** presents the data collected from the experimental phases. It analyzes fresh concrete properties such as slump and workability, mechanical performance metrics including flexural toughness and compressive strength, and the structural load-deflection behavior of the hybrid beam systems.
- **Chapter 5: Conclusions and Recommendations** summarizes the key findings of the study, such as the 0.5% fiber volumetric threshold and the 272% increase in flexural strength for reinforced FRC. It concludes with practical recommendations for future field implementation and identifies areas for further research in fatigue and durability engineering.

Chapter 2:Literature Review

2-1- The Durability Crisis of Reinforced Concrete

The primary challenge facing bridge infrastructure in cold climates is the degradation of concrete durability. While concrete is an excellent load-bearing material, its porous nature and low tensile strength make it susceptible to environmental factors that lead to premature failure.

2-1-1- Chemical and Environmental Degradation

Research identifies several key mechanisms that compromise the integrity of bridge decks:

- Alkali-Silica Reaction (ASR): This chemical reaction occurs between the hydroxyl ions in the cement paste and the silica in certain aggregates, forming a gel that expands upon moisture absorption, leading to internal cracking (Figueira et al., 2019).
- Freeze-Thaw Cycling: In regions like the Northeast U.S., water infiltrates concrete pores. As temperatures drop, the water expands by roughly 9%, creating internal hydraulic pressures that cause micro-cracking and surface scaling (Luo et al., 2017).
- Carbonation: Carbon dioxide (CO_2) from the atmosphere reacts with calcium hydroxide to form calcium carbonate, lowering the concrete's pH. This acidity destroys the passive protective layer around steel reinforcement, initiating corrosion (Papadakis et al., 1991).

2-1-2- Chloride-Induced Corrosion

The most critical threat in cold climates is the ingress of chloride ions from de-icing salts. These salts penetrate the concrete and reach the steel rebar, causing a volume expansion of up to six times the original metal as rust forms. This expansive pressure causes delamination and spalling. With the direct cost of bridge corrosion estimated at $10 billion annually, the shift toward non-corrosive alternatives has become a structural necessity (Yunovich & Thompson, 2003).

2-2- Fiber-Reinforced Polymer (FRP) Reinforcement

FRP rebars, particularly Glass Fiber-Reinforced Polymer (GFRP), represent a significant technological shift from traditional steel.

2-2-1- Material Characteristics

FRP composites consist of high-strength fibers embedded in a polymer matrix. GFRP is widely utilized due to its high tensile strength (86–90 ksi) and absolute resistance to chloride-induced corrosion (Einde et al., 2003). Unlike steel, which is ductile and exhibits a yield point, GFRP is linear-elastic until failure.

2-2-2- Structural Applications and Limitations

Studies have shown that GFRP-reinforced decks perform well under standard truck loads, often with tensile strains representing less than 0.19% of their ultimate capacity (Benmokrane et al., 2006). However, because GFRP cannot undergo plastic deformation, structures must be designed as over-reinforced. This ensures the concrete crushes before the rebar snaps, providing some visual warning of failure.

2-3- Fiber-Reinforced Concrete (FRC)

The integration of fibers into the concrete matrix (FRC) aims to improve the material's inherent weaknesses—specifically its low tensile strength and brittle failure mode.

2-3-1- Role of Basalt Fibers (Minibars)

Basalt fibers are an environmentally sustainable alternative to steel or synthetic fibers. They provide high resistance to acid and salt corrosion.

- Pre-Cracking: Fibers act as fillers, increasing initial compressive and tensile strength (Alaskar et al., 2021).
- Post-Cracking (Toughness): Basalt "minibars" bridge cracks as they form, preventing rapid propagation. Jalasutram et al. (2016) noted that a 2.0% volumetric fraction

of basalt fibers could increase flexural toughness by nearly three times compared to plain concrete.

2-3-2- Synergy Between FRC and GFRP

A critical area of research is the combination of FRC and GFRP rebars. Recent studies suggest that the "crack-bridging" of fibers complements the brittle nature of GFRP. For instance, Meda et al. (2019) found that adding GFRP rebars to an FRC system increased peak load by 63% and reduced crack widths by 60%. This hybrid approach creates a "Steel-Free" system that is both corrosion-resistant and sufficiently ductile for bridge applications.

Chapter 3:Methodology

3-1- Materials

The development of a steel-free bridge deck requires a careful selection of non-corrosive components. The materials used in this study include a modified concrete matrix and advanced polymer reinforcements.

3-1-1- Concrete Mix Components

The base concrete mix was adapted from a design used in the Veranda Street Bridge project in Portland, Maine. It consists of:

- **Cement:** Type 1L Portland-limestone cement (ASTM C595).
- **Water-to-Cement Ratio:** Constant at 0.45.
- **Chemical Admixtures:** Master Glenium 7500 (superplasticizer) to maintain workability and Master Air AE2000 for freeze-thaw resistance.
- **Aggregates:** Two sizes of coarse aggregates were tested: 3/4-inch (angular) and 3/8-inch (rounded).

Table 1. Coarse Aggregates Sieve Analysis

Sieve	% Passing	Limits	MDOT
1"	100.00%	100%	100.00%
3/4"	98.76%	90-100%	97.00%
1/2"	68.16%	-	54.00%
3/8"	36.57%	20-55%	32.00%
#4	2.49%	0-10%	8.00%
#8	0.50%	0-5%	4.00%

Table 2. Fine Aggregate Sieve Analysis

Sieve	% Passing	Limits	MDOT
1"	100.00%	100%	100.00%
3/4"	98.76%	90-100%	97.00%
1/2"	68.16%	-	54.00%
3/8"	36.57%	20-55%	32.00%
#4	2.49%	0-10%	8.00%
#8	0.50%	0-5%	4.00%

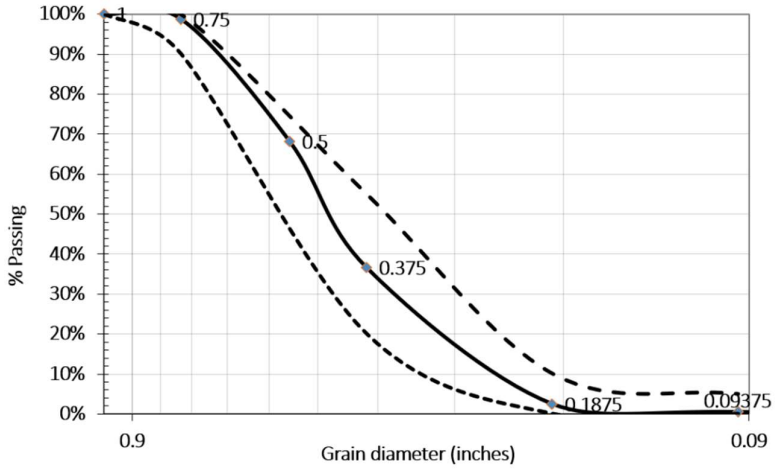

Figure 1.Sieve Analysis Verification for Coarse Aggregates

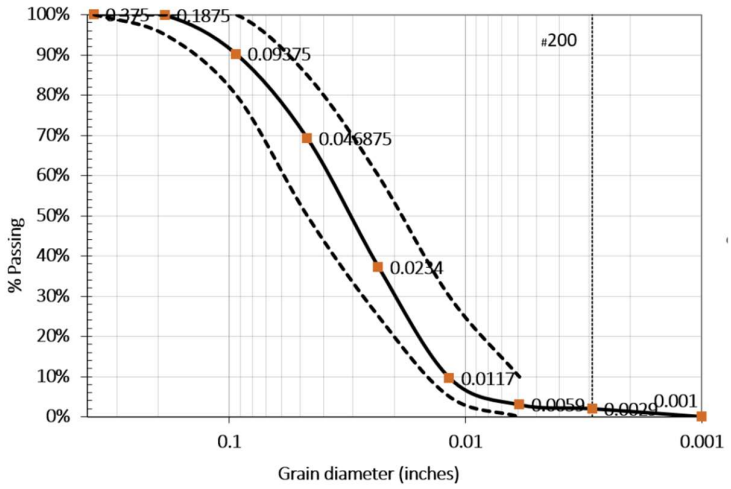

Figure 2. Sieve Analysis Verification for Fine Aggregates

3-1-2- Basalt Fibers (Minibars)

The study utilized basalt "minibars" as secondary reinforcement. Unlike bundled dispersion fibers, minibars are designed to enhance post-cracking toughness by bridging cracks across the concrete matrix.

Table 3. Mix design

Materials	1	2	3	4	5	6	7	8	9	10	11
Cement (lb/yd3)	573	573	573	573	573	573	573	573	573	573	573
3/4" Coarse (lb/yd3)	1749	1749	1749	1749	1749	1749	-	-	-	-	-
3/8" Coarse (lb/yd3)	-	-	-	-	-	-	1749	1749	1749	1749	1749
Fine (lb/yd3)	1063	1063	1063	1063	1063	1063	1063	1063	1063	1063	1063
Masterair AE200 (oz/yd3)	1.75	1.75	1.75	1.75	1.75	1.75	1.75	1.75	1.75	1.75	1.75
MasterGlenium 7500 (oz/yd3)	29.7	32.5	38.9	67.5	75.4	99.2	29.7	38.9	67.5	69.4	99.2
Fibers (vol%)	0%	0.1%	0.2%	0.5%	1.0%	1.2%	0%	0.2%	0.5%	0.8%	1.2%

3-1-3- GFRP Rebars

For primary reinforcement in Phase 2, #4 Glass Fiber-Reinforced Polymer (GFRP) rebars were used. These bars are characterized by high tensile strength (approx. 90 ksi) but a lower modulus of elasticity compared to steel, requiring a specific design approach to manage deflection.

Table 4. Material Properties

Properties	Values (Ksi)
f'c	6

Ec	4700
fu	90
E_f	5900

3-2- Test Setup & Process

3-2-1- Specimen Fabrication and Casting Protocol

The integrity of the experimental results relied on a rigorous and repeatable casting procedure. Specimens were fabricated in three distinct geometries to facilitate specific mechanical evaluations:

- **Flexural Specimens:** 6" x 6" x 22" beams (Phase 1) and 4" x 4" x 54" beams (Phase 2).
- **Compressive Specimens:** 4" x 8" cylinders.
- **Shrinkage Specimens:** 3" x 3" x 11.25" prisms with embedded shrinkage bolts.

2.2.1 Standardized Mixing Procedure

The mixing sequence was adapted from the Maine Department of Transportation (MDOT) protocols to ensure the homogeneity of the Basalt Fiber-Reinforced Concrete (BFRC). To prevent "balling" of fibers and to ensure full hydration, the following step-by-step laboratory protocol was established:

1. **Batch Limitation:** Batch sizes were restricted to 50% of the mixer's rated capacity to ensure high-shear mixing and uniform fiber distribution.
2. **Moisture Correction:** Aggregate moisture content was measured immediately prior to mixing, and batch water was adjusted to maintain a precise w/c ratio of 0.45.
3. **Pre-Conditioning:** The drum was "buttered" with a specialized slurry to prevent the loss of fines to the mixer blades.
4. **Sequential Addition:** Aggregates and 50% of the water/air-entraining agent were mixed for 3 minutes, followed by a 3-minute rest.
5. **Chemical Activation:** Cement and the remaining water, containing roughly 90% of the predicted superplasticizer, were added and mixed for an additional 3 minutes.

6. **Workability Verification:** A slump test was performed per **ASTM C143**. If the 3-inch target was not met, superplasticizer was added in 0.1 oz increments.
7. **Fiber Integration:** Basalt fibers were introduced while the mixer was operational. A final 2-minute mix and 1-minute rest were enforced to ensure the fibers were fully encapsulated by the cement paste.
8. **Time Constraints:** All casting and vibration were completed within a 25-minute window from initial hydration to prevent the negative effects of premature setting.

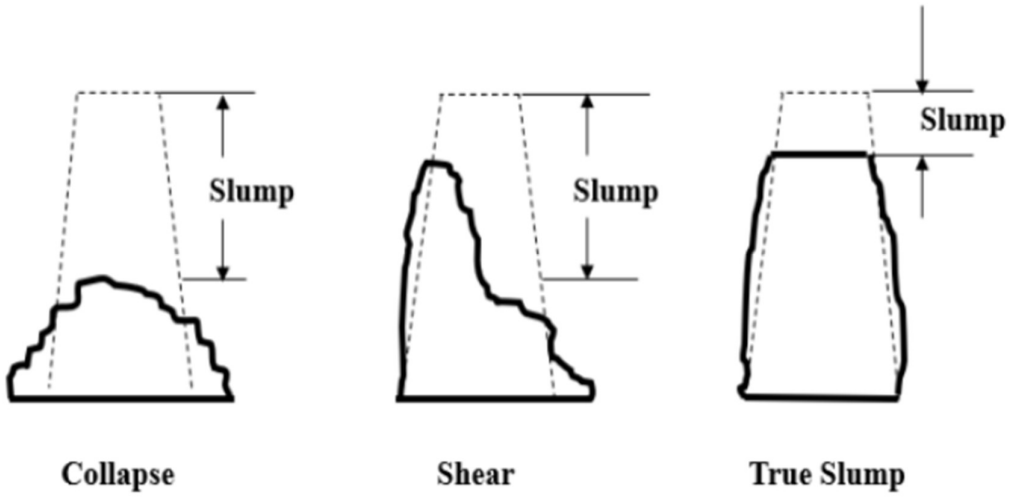

Figure 3. Different types of slumps. (Ferraris & de Larrard, 1998)

This figure is vital to explain why the 0.5% fiber threshold was chosen based on the transition from "True" to "Shear" slump.

3-2-2- Consolidation and Curing

Upon casting, all specimens were placed on a vibration table for approximately 30 seconds. This step was critical for fiber-reinforced mixes to eliminate entrapped air and prevent fiber "clustering." Specimens were cured in a controlled environmental chamber (wet room) at 98% humidity and a constant temperature. Demolding occurred at 24 hours, with testing performed at 28 days for Phase 1 and 60+ days for Phase 2.

3-3- Phase 1: Material Performance Testing Setup

To define the baseline properties of the BFRC, the following standardized test configurations were utilized:

3-3-1- Flexural Strength (Three-Point Bending)

Tests were conducted per **ASTM C78** using a high-capacity Instron load frame.

- **Span:** 19-inch clear span with 1.5-inch overhangs.
- **Loading Rate:** A constant rate of 0.2 in/min was applied.
- **Objective:** To determine the Modulus of Rupture (MOR) and the post-peak energy absorption (toughness) provided by varying fiber volumes.

Figure 4. Flexure Test Setup (Three-Point)

3-3-2- Compressive Strength and Modulus

Testing was performed per **ASTM C39**. Specimens were capped with neoprene pads within steel bearing blocks to ensure uniform load distribution and to mitigate stress concentrations caused by minor surface irregularities.

- **Loading Rate:** 20 to 50 psi/sec.

Figure 5. Compression Test Setup

3-3-3- Drying Shrinkage Evaluation

Following **ASTM C157**, longitudinal changes were measured using a length comparator and a 10-inch digital dial gage. Readings were taken daily for 30 days to quantify how basalt fibers restrict the volumetric contraction of the cement paste.

3-4- Phase 2: Structural Beam Testing and Instrumentation

The second phase transitioned from material samples to structural members, integrating GFRP rebars into the BFRC matrix.

3-4-1- Primary Reinforcement Preparation

#4 GFRP rebars were utilized. To ensure sufficient development length (Ld), the bars were bent using a controlled heat-treatment process.

- **Bending Process:** A heat gun was used to uniformly warm a 5-inch section of the bar. The bars were then bent around a 4-inch diameter mandrel to prevent "kinking" or fiber breakage.
- **Placement:** Rebars were secured at an effective depth (d) of 2.5 inches (1.5-inch clear cover) using steel wire ties.

Figure 6. Wood Mold (left) and PETG Rebars Before Bending (right)

Figure 7. PETG Rebars Placed in Molds Prior to Casting

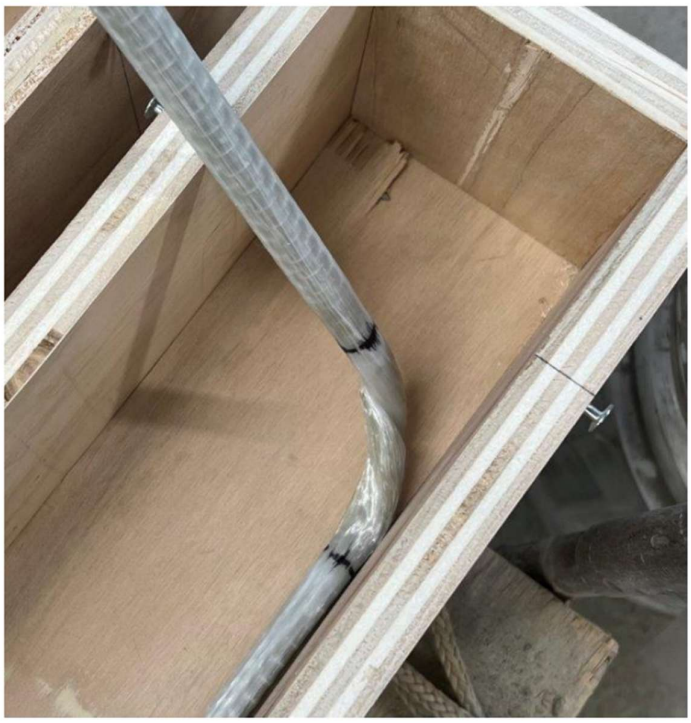

Figure 8. PETG Rebar Bend Profile

3-4-2- Four-Point Bending Configuration

A four-point bending setup was selected per **ASTM C1609** to create a zone of constant maximum moment between the two loading points. This setup minimizes shear influence and allows for a clearer evaluation of the flexural synergy between the fibers and the GFRP rebars.

- **Support Structure:** A W8x13 steel I-beam was used as a rigid base to eliminate support deflection.
- **Loading Fixture:** A custom 1-inch thick steel spreader plate was designed to transfer the Instron's load to the one-third points of the 48-inch span.
- **Instrumentation Suite: * String Potentiometers:** Positioned at mid-span to record deflection.
    - **Acoustic Emission (AE) Sensors:** Attached to the beam surface to monitor the onset of internal micro-cracking and fiber pull-out.
    - **Go-Pro Video:** Used for visual crack propagation mapping.
-

Figure 9. Final Test Setup

3-5- Quality Control and Calibration

Before full-scale testing, a "Mock Test" was conducted on a 6" x 6" beam to calibrate the data acquisition system and fine-tune the AE sensor thresholds. This ensured that the transition from elastic behavior to concrete crushing was captured with high resolution.

Figure 10. Mock Test Setup

Chapter 4:Results and Discussion

4-1- Fresh Concrete Properties: Slump and Workability

Workability is a critical factor for the field application of Fiber-Reinforced Concrete (FRC). For this study, a target slump of **3 inches** was established to ensure that the mix could be effectively placed in bridge deck applications.

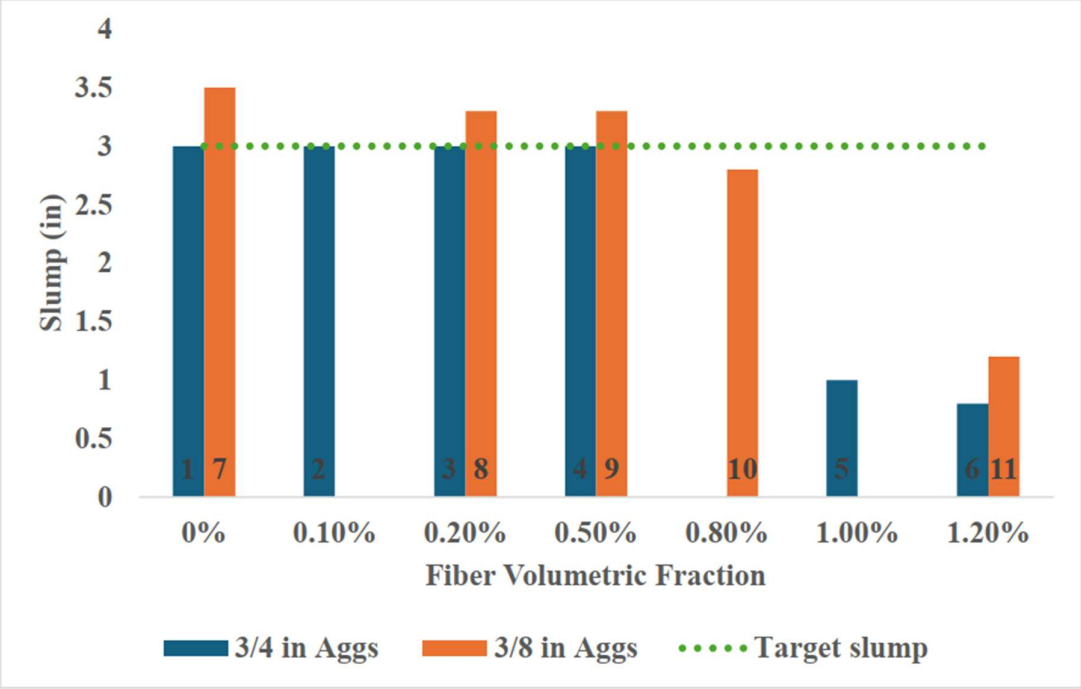

Figure 11. Slump Test Results for Mix Designs

As illustrated in **Figure 11**, the inclusion of basalt fibers significantly impacts the slump of the concrete. Key observations include:

- **The 0.5% Threshold:** A "True Slump" of 3 inches was maintainable up to a fiber content of 0.5% volumetric fraction. Beyond this point, the mix became "fiber-heavy," and additional superplasticizer resulted in a watery consistency without improving the actual slump.
- **Fiber Volume Impact:** Comparing Mix 4 (0.5% fibers) to Mix 6 (1.2% fibers) revealed a **73% decrease in slump**, indicating a severe loss of workability.

- **Aggregate Morphology:** On average, the 3/8-inch aggregate mixes showed a **22% higher slump** than the 3/4-inch mixes. This is attributed to the rounded shape and smaller size of the 3/8-inch aggregates, which facilitate better movement of the 1.7-inch long fibers within the matrix.

4-2- Mechanical Performance (Phase 1)

4-2-1- Three-Point Bending and Flexural Strength

Three-point bending tests were conducted on 11 unique mix designs to analyze how fibers enhance the tensile capacity and toughness of the concrete.

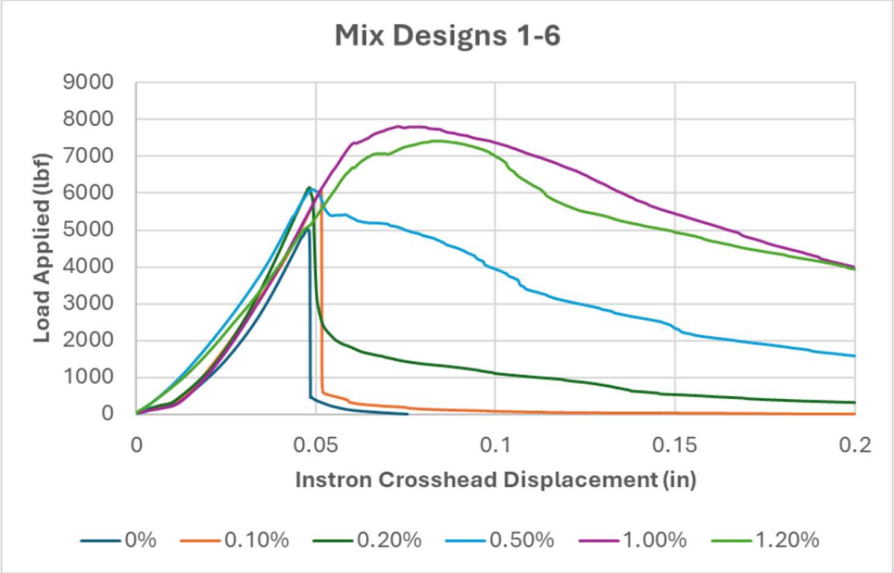

Figure 12. Load vs. Crosshead Displacement for 3/4-inch Aggregates

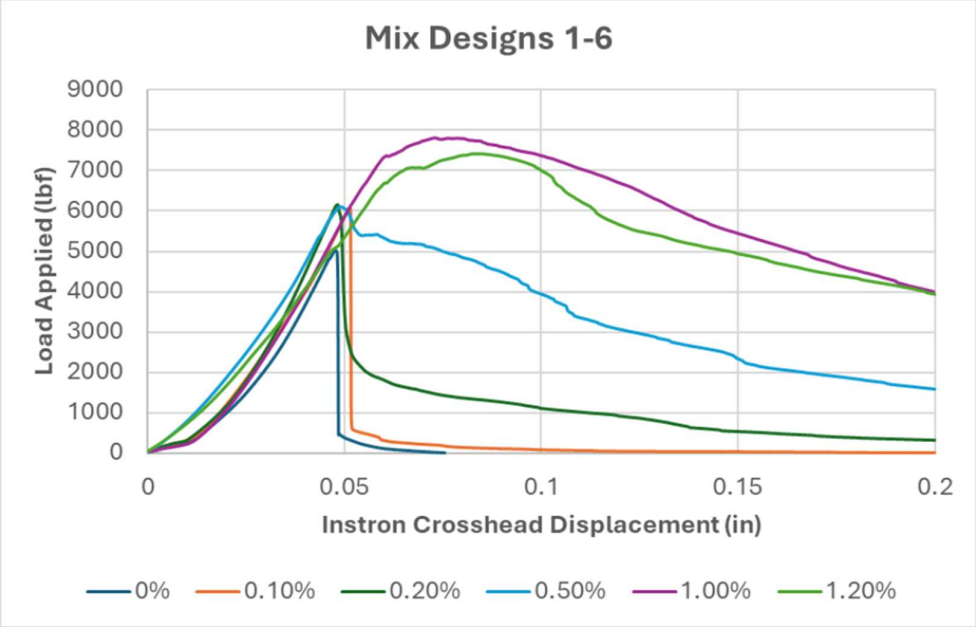

Figure 13. Load vs. Crosshead Displacement for 3/8-inch Aggregates

The load-displacement curves in **Figures 12 and 13** demonstrate that while the initial elastic slope remains similar across mixes, the peak load and post-peak behavior change drastically with fiber content:

- **Peak Strength:** A clear trend of increased flexural strength was observed with higher fiber fractions. The highest capacity was reached at 1.0% fiber content, showing an average strength of **1011 psi**—a **40% increase** over the base concrete (678 psi).
- **Aggregate Impact:** The angular 3/4-inch aggregates provided roughly 5% higher strength than the rounded 3/8-inch aggregates at lower fiber dosages. However, at the 1.2% dosage, the 3/8-inch mix outperformed the 3/4-inch mix due to better workability and fiber homogenization during casting.

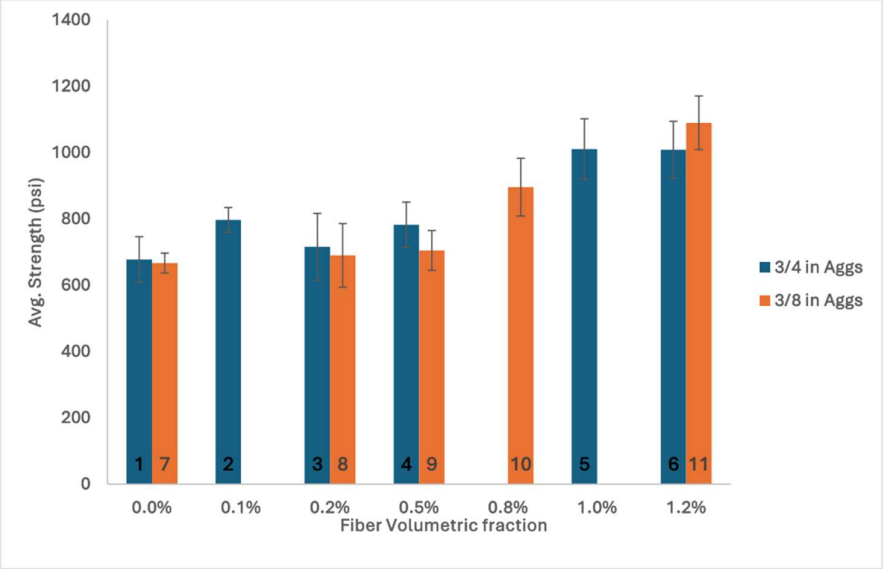

Figure 14. Average Flexural Strength of Specimens

4-2-2- Energy Absorption and Toughness

A primary advantage of adding basalt fibers is the transition from brittle to ductile failure. This is quantified by evaluating **Strain Energy (SE)** in the pre-peak and post-peak regions.

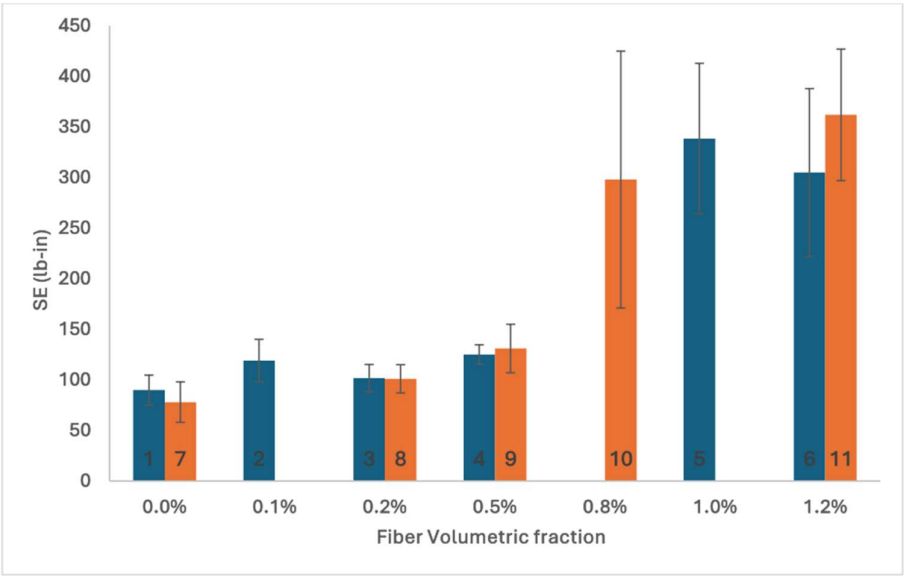

Figure 15.Pre-Peak Strain Energy

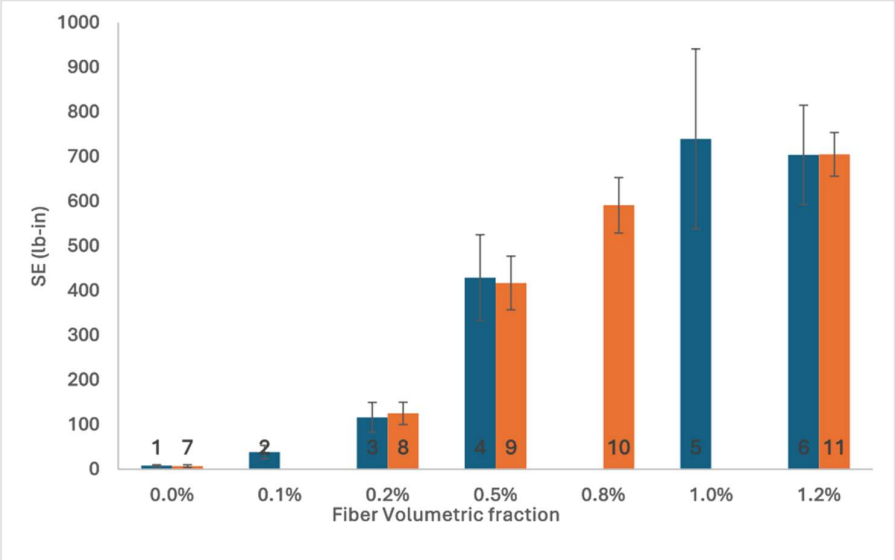

Figure 16.Post-Peak Strain Energy

- **Post-Peak Toughness:** As seen in **Figure 16**, post-peak strain energy rose from nearly zero in plain concrete to **700 lbs-inch** at 1.2% fiber content. This is due to the "crack-bridging" effect of the minibars, which maintain load-carrying capacity even after the concrete matrix has ruptured.
- **Variability:** Larger error bars were noted at higher fiber contents (above 0.5%), suggesting that maintaining 100% homogeneity becomes difficult in highly dense fiber mixes.

4-2-3- Shrinkage Resistance

Shrinkage is a primary cause of early-age cracking in bridge decks. **Figure 17** displays the 28-day shrinkage strain results.

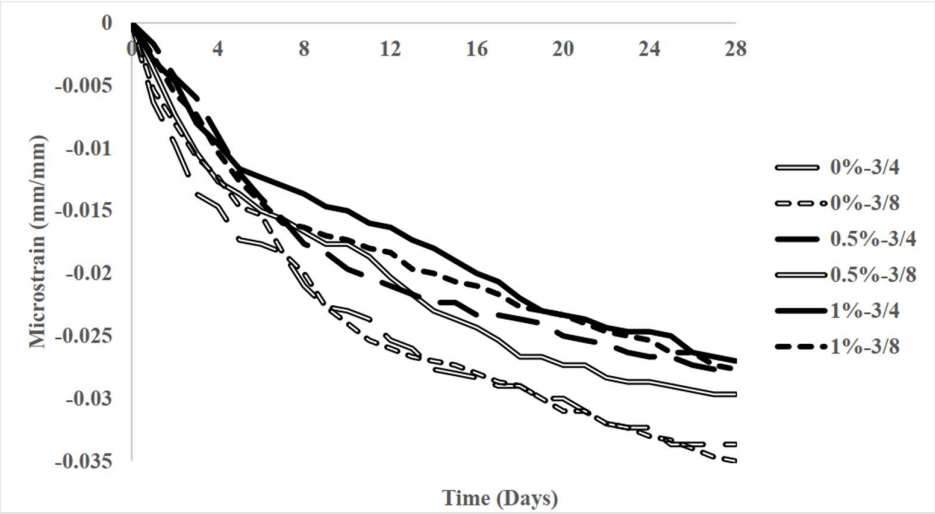

Figure 17. 28-day Shrinkage Test Data

The results indicate that fibers serve as an internal constraint, reducing shrinkage strain by **20% to 21%** at 1.0% fiber content compared to the control. However, the improvement between 0.5% and 1.0% was marginal (2-5%), suggesting a law of diminishing returns for shrinkage mitigation.

4-3- Compressive Strength Analysis

Compressive tests (ASTM C39) were conducted to ensure the mix met the design requirement of **6 ksi**.

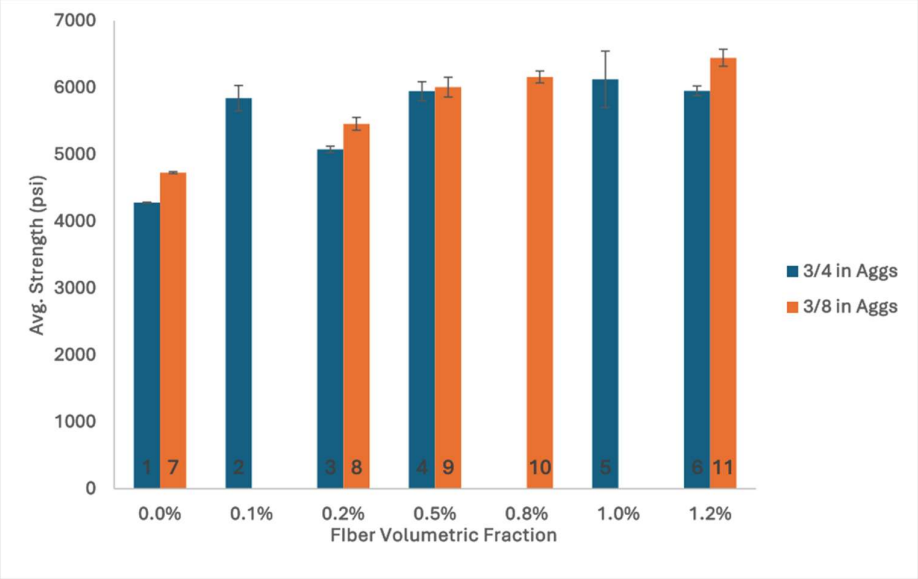

Figure 18. Compression Test Data for Mix Designs 1-11

- **Strength Gain:** Compressive capacity increased up to the 0.5% fiber content mark (**39% increase** for 3/4-inch aggregates). Beyond 0.5%, the strength plateaued, with only a 0.1% to 7.6% increase observed at the 1.2% dosage level.
- **Secondary Testing (Phase 2 Validation):** A second set of cylinders was tested to validate the Phase 2 casting.

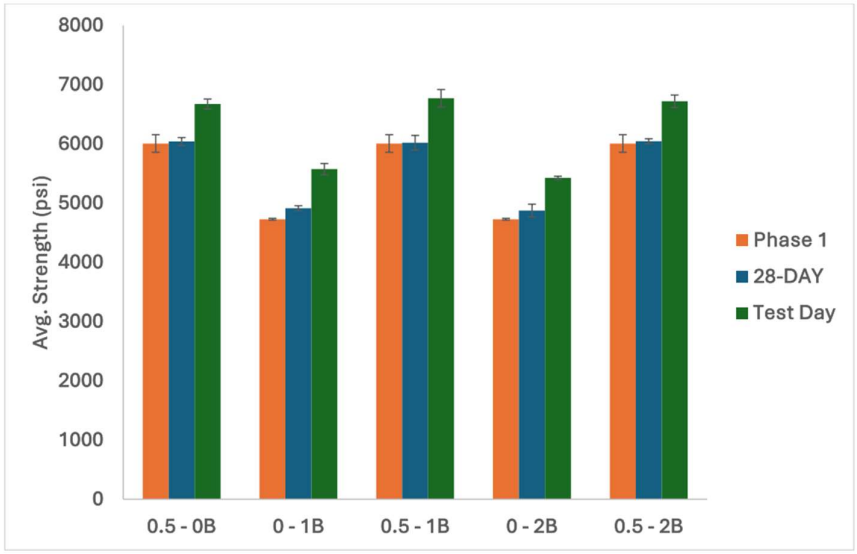

Figure 19. Phase 1 and Phase 2 Compression Data Comparison

As shown in **19**, specimens tested on the day of the flexure tests (60+ days) showed a **10.5% increase** in strength over the 28-day results. This confirms that the mixing procedure remained consistent across different batching phases.

4-4- Structural Response (Phase 2): GFRP-Reinforced Beams

Phase 2 combined the optimized 0.5% BFRC mix with GFRP rebars in a four-point bending setup.

4-4-1- Load-Deflection Behavior

The load-deflection curves in **Figure 20** highlight the synergy between the fiber-reinforced matrix and the primary GFRP reinforcement.

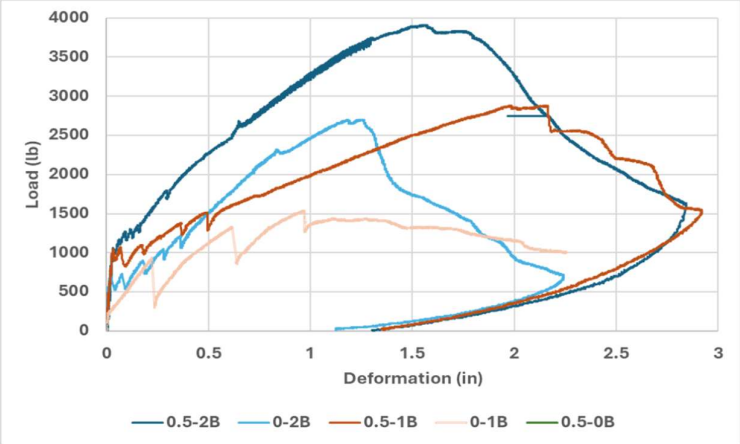

Figure 20.Load Applied vs. Mid-span Deflection

- **Ductility and Peak Load:** Plain concrete beams with one GFRP rebar peaked at a deflection of 0.97 inches. In contrast, the BFRC beams with one rebar peaked at **2.16 inches**, demonstrating exceptional ductility and energy absorption.
- **Crack Control:** While GFRP-reinforced beams typically exhibit large, concentrated cracks, the inclusion of fibers resulted in multiple, smaller cracks distributed along the beam span.

4-4-2- Comparative Flexural Strength

The flexural strength for the hybrid system is summarized in **Figure 21**.

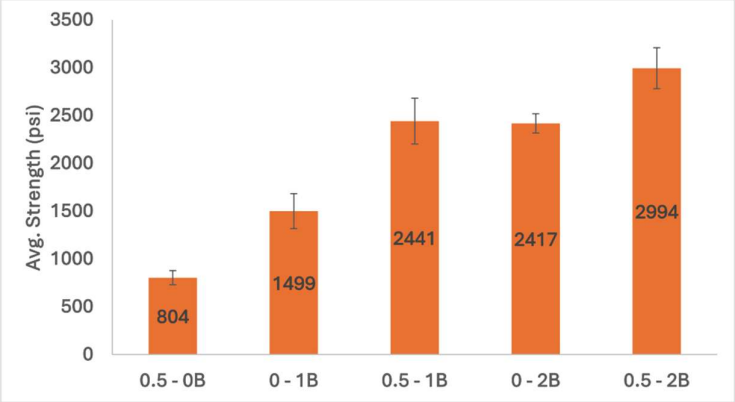

Figure 21. Flexural Strength of Specimens

- **Reinforcement Impact:** Adding 0.5% fibers to a 1-rebar system increased flexural strength by **63%** compared to the plain concrete counterpart.
- **The "One vs. Two Rebar" Comparison:** An essential finding was that the **0.5% Fiber + 1-Rebar** specimen performed virtually identically (within 1%) to the **Plain Concrete + 2-Rebar** specimen in terms of strength, but with much higher deflection and ductility. This indicates that fibers can partially offset the need for higher rebar counts while improving the failure mode of the structure.

Chapter 5:Conclusions and Recommendations

5-1- Summary of Findings

This research successfully characterized 11 unique BFRC mix designs and validated their structural performance through large-scale beam testing. The investigation utilized a two-phase methodology to balance material optimization with structural utility, adhering to **AASHTO LRFD Bridge Design Guide Specifications**.

5-1-1- Phase 1: Material Optimization

The initial phase confirmed that basalt fibers significantly enhance the mechanical properties of concrete, but introduce a critical workability threshold.

- **Workability Limit:** A fiber content of **0.5% by volume** was identified as the optimal threshold. Beyond this, slump values dropped by up to **73%**, creating a "fiber-heavy" mix that is difficult to pump and consolidate.
- **Mechanical Gains:** The 1.0% fiber content provided the highest flexural strength (**1011 psi**, a **40% increase** over control) and a **39% increase** in compressive capacity.
- **Aggregate Selection:** Smaller, rounded **3/8-inch aggregates** yielded **22% better workability** and more consistent fiber distribution compared to larger angular aggregates.
- **Shrinkage Control:** Fibers effectively acted as internal constraints, reducing 28-day shrinkage strain by **21%**.

5-1-2- Phase 2: Structural Synergy

The combination of BFRC and GFRP primary reinforcement successfully mitigated the brittle failure modes typically associated with FRP materials.

- **Flexural Performance:** A massive **272% increase** in flexural strength was achieved by combining the 0.5% FRC mix with a 2-bar GFRP system compared to unreinforced FRC.

- **Ductility and Energy Absorption:** The most significant benefit was observed in 1-bar systems, where fibers increased peak deflection from **0.97 inches to 2.16 inches**. This shift represents a transition from sudden brittle failure to a more ductile, predictable response.
- **Design Efficiency:** Notably, the **0.5% fiber + 1-bar** specimen achieved nearly the same strength as a **plain concrete + 2-bar** specimen, suggesting that fibers can optimize reinforcement ratios while providing superior crack control.

5-2- Conclusions

The study demonstrates that a **"Steel-Free"** system is mechanically viable. The inclusion of basalt fibers bridges micro-cracks and maintains load-carrying capacity even after initial rupture, effectively overcoming the primary structural disadvantage of GFRP (brittleness). However, the increased deflection observed in GFRP systems remains higher than that of traditional steel. While the materials meet strength requirements, the lower stiffness of the GFRP bars used in this study suggests that serviceability limits (deflection control) must be a primary focus in future design iterations.

5-3- Recommendations for Future Work

To advance this technology toward commercial bridge deck applications, the following research paths are recommended:

1. **Workability Engineering:** Investigate the use of high-range water reducers or various fiber aspect ratios to increase the 0.5% volumetric threshold, allowing for higher fiber densities without sacrificing pumpability.
2. **Fatigue and Cyclic Loading:** Bridge decks undergo millions of load cycles. Testing the fatigue life of the BFRC-GFRP bond is essential to ensure long-term structural integrity.
3. **Durability in Harsh Environments:** Conduct accelerated aging tests to evaluate the alkaline resistance of basalt fibers within the concrete matrix over a simulated 50-year service life.

4. **Codification and Stiffness:** Engineer GFRP rebars with higher moduli of elasticity to align more closely with AASHTO stiffness requirements, thereby reducing the mid-span deflection levels observed in this study.

Acknowledgments

The authors gratefully acknowledge the support and funding provided by the Transportation Infrastructure Durability Center (TIDC), the Maine Department of Transportation (MDOT), and the Advanced Structures and Composites Center (ASCC), which were crucial in facilitating this research. Special thanks are also extended to the Civil Engineering Department of the University of Maine for their support throughout this study.

References:

Abbass, W., Khan, M., & Mourad, S. (2018). Evaluation of mechanical properties of steel fiber reinforced concrete with different strengths of concrete. Construction and Building Materials, 168, 556-569. https://doi.org/10.1016/J.CONBUILDMAT.2018.02.164.

Aguiar, J., & Júnior, C. (2013). Carbonation of surface protected concrete. Construction and Building Materials, 49, 478-483. https://doi.org/10.1016/J.CONBUILDMAT.2013.08.058.

Ai, C., Rahman, A., Wang, F., Yang, E., & Qiu, Y. (2017). Experimental study of a new modified waterproof asphalt concrete and its performance on bridge deck. Road Materials and Pavement Design, 18, 270-280. https://doi.org/10.1080/14680629.2017.1329881.

Alaskar, A., Albidah, A., Alqarni, A., Alyousef, R., & Mohammadhosseini, H. (2021). Performance evaluation of high-strength concrete reinforced with basalt fibers exposed to elevated temperatures. Journal of Building Engineering, 35, 102108. https://doi.org/10.1016/j.jobe.2020.102108.

Al-Mufti, R., & Fried, A. (2016). Pulse velocity assessment of early age creep of concrete. Construction and Building Materials, 121, 622-628. https://doi.org/10.1016/J.CONBUILDMAT.2016.06.015.

American Association of State Highway and Transportation Officials. (2018). AASHTO LRFD bridge design specifications (2nd ed.). American Association of State Highway and Transportation Officials.

American Concrete Institute. (2010). ACI 212.3R-10: Report on chemical admixtures for concrete. American Concrete Institute.

American Concrete Institute. (2015). ACI 440.1R-15: Guide for the design and construction of structural concrete reinforced with FRP bars. American Concrete Institute.

American Concrete Institute. (2019). ACI 318-19: Building code requirements for structural concrete and commentary. American Concrete Institute.

ASTM International. (2015). ASTM C78/C78M-15: Standard test method for flexural strength of concrete (using simple beam with third-point loading). ASTM International.

ASTM International. (2015). Standard test method for slump of hydraulic-cement concrete (ASTM C143-15). ASTM International.

ASTM International. (2021). Standard specification for concrete aggregates (ASTM C33-21). ASTM International.

ASTM International. (2021). Standard test method for relative density (specific gravity) and absorption of coarse aggregate (ASTM C127-21). ASTM International.

ASTM International. (2021). Standard test method for relative density (specific gravity) and absorption of fine aggregate (ASTM C128-21). ASTM International.

ASTM International. (2024). ASTM C39/C39M-24: Standard test method for compressive strength of cylindrical concrete specimens. ASTM International.

ASTM International. (2024). ASTM C157/C157M-24: Standard test method for length change of hardened hydraulic-cement mortar and concrete. ASTM International.

ASTM International. (2024). ASTM C1609/C1609M-24: Standard test method for flexural performance of fiber-reinforced concrete (using beam with third-point loading). ASTM International.

Benmokrane, B., El-Salakawy, E., El-Ragaby, A., & Lackey, T. (2006). Designing and Testing of Concrete Bridge Decks Reinforced with Glass FRP Bars. Journal of Bridge Engineering, 11, 217-229. https://doi.org/10.1061/(ASCE)1084-0702(2006)11:2.(217)

Branston, J., Das, S., Kenno, S., & Taylor, C. (2016). Mechanical behaviour of basalt fibre reinforced concrete. Construction and Building Materials, 124, 878-886. https://doi.org/10.1016/J.CONBUILDMAT.2016.08.009.

Caratelli, A., Meda, A., Rinaldi, Z., Spagnuolo, S., & Maddaluno, G. (2017). Optimization of GFRP reinforcement in precast segments for metro tunnel lining. Composite Structures, 181, 336-346. https://doi.org/10.1016/J.COMPSTRUCT.2017.08.083.

Carballosa, P., Calvo, J., & Revuelta, D. (2020). Influence of expansive calcium sulfoaluminate agent dosage on properties and microstructure of expansive self-compacting concretes. Cement & Concrete Composites, 107, 103464. https://doi.org/10.1016/j.cemconcomp.2019.103464.

Choumanidis, D., Badogiannis, E., Nomikos, P., & Sofianos, A. (2016). The effect of different fibres on the flexural behaviour of concrete exposed to normal and elevated temperatures. Construction and Building Materials, 129, 266-277. https://doi.org/10.1016/J.CONBUILDMAT.2016.10.089.

Cuelho, E., Stephens, J., Smolenski, P., & Johnson, J. (2006). Evaluating Concrete Bridge Deck Performance. https://doi.org/10.21949/151819066.

Einde, L., Zhao, L., & Seible, F. (2003). Use of FRP composites in civil structural applications. Construction and Building Materials, 17, 389-403. https://doi.org/10.1016/S0950-0618(03)00040-0.

Elahi, M., Shearer, C., Reza, A., Saha, A., Khan, M., Hossain, M., & Sarker, P. (2021). Improving the sulfate attack resistance of concrete by using supplementary cementitious materials (SCMs): A review. Construction and Building Materials, 281, 122628. https://doi.org/10.1016/J.CONBUILDMAT.2021.122628.

Erki, M., & Rizkalla, S. (1993). FRP Reinforcement for Concrete Structures. Concrete International, 15, 48-53.

Esposito, R., Anaç, C., Hendriks, M., & Çopuroğlu, O. (2016). Influence of the Alkali-Silica Reaction on the Mechanical Degradation of Concrete. Journal of Materials in Civil Engineering, 28, 04016007. https://doi.org/10.1061/(ASCE)MT.1943-5533.0001486.

Ferraris, C. and DeLarrard, F. (1998). Testing and Modeling of Fresh Concrete Rheology, NIST Interagency/Internal Report (NISTIR), National Institute of Standards and Technology, Gaithersburg, MD. https://doi.org/10.6028/NIST.IR.6094.

Figueira, R., Sousa, R., Coelho, L., Azenha, M., Almeida, J., Jorge, P., & Silva, C. (2019). Alkali-silica reaction in concrete: Mechanisms, mitigation and test methods. Construction and Building Materials. https://doi.org/10.1016/J.CONBUILDMAT.2019.07.230.

Fořt, J., Kočí, J., & Černý, R. (2021). Environmental Efficiency Aspects of Basalt Fibers Reinforcement in Concrete Mixtures. Energies, 14, 7736. https://doi.org/10.3390/en14227736.

Gori, R. (1999). Theoretical Performances of RC Elements Built at Turn of the Century. Journal of Performance of Constructed Facilities, 13, 57-66. https://doi.org/10.1061/(ASCE)0887-3828(1999)13:2.(57)

Goyal, A., Pouya, H., Ganjian, E., & Claisse, P. (2018). A Review of Corrosion and Protection of Steel in Concrete. Arabian Journal for Science and Engineering, 43, 5035-5055. https://doi.org/10.1007/S13369-018-3303-2.

Helba, A. (1944). Reinforced Concrete Structures. Nature, 154, 502-502. https://doi.org/10.1038/154502a0.

Holden, K., Pantelides, C., & Reaveley, L. (2014). Bridge Constructed with GFRP-Reinforced Precast Concrete Deck Panels: Case Study. Journal of Bridge Engineering, 19, 05014001. https://doi.org/10.1061/(ASCE)BE.1943-5592.0000589.

Jia, X., Huang, B., Chen, S., & Shi, D. (2016). Comparative investigation into field performance of steel bridge deck asphalt overlay systems. KSCE Journal of Civil Engineering, 20, 2755-2764. https://doi.org/10.1007/S12205-016-0259-1.

Junaid, M., Elbana, A., Altoubat, S., & Al-Sadoon, Z. (2019). Experimental study on the effect of matrix on the flexural behavior of beams reinforced with Glass Fiber Reinforced Polymer (GFRP) bars. Composite Structures. https://doi.org/10.1016/J.COMPSTRUCT.2019.110930.

Kaplan, M. (1958). The effects of the properties of coarse aggregates on the workability of concrete. Magazine of Concrete Research, 10, 63-74. https://doi.org/10.1680/MACR.1958.10.29.63.

Karim, R., & Shafei, B. (2021). Performance of fiber-reinforced concrete link slabs with embedded steel and GFRP rebars. Engineering Structures, 229, 111590. https://doi.org/10.1016/j.engstruct.2020.111590.

Kim, Y., Lee, K., Bang, J., & Kwon, S. (2014). Effect of W/C Ratio on Durability and Porosity in Cement Mortar with Constant Cement Amount. Advances in Materials Science and Engineering, 2014, 1-11. https://doi.org/10.1155/2014/273460.

Kirthika, S., & Singh, S. (2018). Experimental Investigations on Basalt Fibre-Reinforced Concrete. Journal of The Institution of Engineers (India): Series A, 99, 661-670. https://doi.org/10.1007/S40030-018-0325-4.

Kizilkanat, A., Kabay, N., Akyuncu, V., Chowdhury, S., & Akca, A. (2015). Mechanical properties and fracture behavior of basalt and glass fiber reinforced concrete: An experimental study. Construction and Building Materials, 100, 218-224. https://doi.org/10.1016/J.CONBUILDMAT.2015.10.006.

Lai, M., Binhowimal, S., Griffith, A., Hanžič, L., Wang, Q., Chen, Z., & Ho, J. (2021). Shrinkage design model of concrete incorporating wet packing density. Construction and Building Materials, 280, 122448. https://doi.org/10.1016/J.CONBUILDMAT.2021.122448.

Liu, Q., Su, R., & Xu, F. (2021). Quantification of the actual expansion and deposition of rust in reinforced concrete. Construction and Building Materials, 297, 123760. https://doi.org/10.1016/J.CONBUILDMAT.2021.123760.

Luo, Q., Liu, D., Qiao, P., Feng, Q., & Sun, L. (2017). Microstructural damage characterization of concrete under freeze-thaw action. International Journal of Damage Mechanics, 27, 1551-1568. https://doi.org/10.1177/1056789517736573.

Makomra, V., et al. (2022). Physico-Mechanical Properties of Bio-Based Bricks. Journal of Materials Science and Chemical Engineering. https://doi.org/10.4236/msce.2022.104002.

Mayercsik, N., Vandamme, M., & Kurtis, K. (2016). Assessing the efficiency of entrained air voids for freeze-thaw durability through modeling. Cement and Concrete Research, 88, 43-59. https://doi.org/10.1016/J.CEMCONRES.2016.06.004.

Meda, A., Rinaldi, Z., Spagnuolo, S., De Rivaz, B., & Giamundo, N. (2019). Hybrid precast tunnel segments in fiber reinforced concrete with glass fiber reinforced bars. Tunnelling and Underground Space Technology. https://doi.org/10.1016/J.TUST.2019.01.016.

Mehta, P. (1983). Mechanism of sulfate attack on portland cement concrete — Another look. Cement and Concrete Research, 13, 401-406. https://doi.org/10.1016/0008-8846(83)90040-6.

Nelson, M., & Fam, A. (2013). Structural GFRP Permanent Forms with T-Shape Ribs for Bridge Decks Supported by Precast Concrete Girders. Journal of Bridge Engineering, 18, 813-826. https://doi.org/10.1061/(ASCE)BE.1943-5592.0000418.

Papadakis, V., Vayenas, C., & Fardis, M. (1991). Experimental investigation and mathematical modeling of the concrete carbonation problem. Chemical Engineering Science, 46, 1333-1338. https://doi.org/10.1016/0009-2509(91)85060-B.

Radocea, A. (1994). A model of plastic shrinkage. Magazine of Concrete Research, 46, 125-132. https://doi.org/10.1680/MACR.1994.46.167.125.

Rajabipour, F., Giannini, E., Dunant, C., Ideker, J., & Thomas, M. (2015). Alkali-silica reaction: Current understanding of the reaction mechanisms and the knowledge gaps. Cement and Concrete Research, 76, 130-146. https://doi.org/10.1016/J.CEMCONRES.2015.05.024.

Rozière, E., Loukili, A., & Cussigh, F. (2009). A performance based approach for durability of concrete exposed to carbonation. Construction and Building Materials, 23, 190-199. https://doi.org/10.1016/J.CONBUILDMAT.2008.01.006.

Russell, H. (2004). CONCRETE BRIDGE DECK PERFORMANCE. NCHRP Synthesis of Highway Practice. https://doi.org/10.17226/17608.

Silu, H., Fu, Q., Yan, L., & Kasal, B. (2021). Characterization of interfacial properties between fibre and polymer matrix in composite materials – A critical review. Journal of Materials Research and Technology. https://doi.org/10.1016/J.JMRT.2021.05.076.

Tan, P., Zhao, Y., & Meng, Q. (2014). Test and Application of High Performance Concrete. Advanced Materials Research, 908, 30-33. https://doi.org/10.4028/www.scientific.net/AMR.908.30.

Torgal, F., Miraldo, S., Labrincha, J., & Brito, J. (2012). An overview on concrete carbonation in the context of eco-efficient construction: Evaluation, use of SCMs and/or RAC. Construction and Building Materials, 36, 141-150. https://doi.org/10.1016/J.CONBUILDMAT.2012.04.066.

Tu, W., Zhu, Y., Fang, G., Wang, X., & Zhang, M. (2019). Internal curing of alkali-activated fly ash-slag pastes using superabsorbent polymer. Cement and Concrete Research. https://doi.org/10.1016/J.CEMCONRES.2018.11.018.

Vandamme, M., & Ulm, F. (2009). Nanogranular origin of concrete creep. Proceedings of the National Academy of Sciences, 106, 10552-10557. https://doi.org/10.1073/pnas.0901033106.

Vinkler, M., & Vitek, J. (2017). Drying shrinkage of concrete elements. Structural Concrete, 18, 103-92. https://doi.org/10.1002/suco.201500208.

Wu, G., Wang, X., Wu, Z., Dong, Z., & Zhang, G. (2015). Durability of basalt fibers and composites in corrosive environments. Journal of Composite Materials, 49, 873-887. https://doi.org/10.1177/0021998314526628.

Wu, L., Farzadnia, N., Shi, C., Zhang, Z., & Wang, H. (2017). Autogenous shrinkage of high performance concrete: A review. Construction and Building Materials, 149, 62-75. https://doi.org/10.1016/J.CONBUILDMAT.2017.05.064.

Xue, Q., Liu, L., Zhao, Y., Chen, Y., & Li, J. (2013). Dynamic behavior of asphalt pavement structure under temperature-stress coupled loading. Applied Thermal Engineering, 53, 1-7. https://doi.org/10.1016/J.APPLTHERMALENG.2012.10.055.

Yunovich, M., & Thompson, N. (2003). CORROSION OF HIGHWAY BRIDGES: ECONOMIC IMPACT AND CONTROL METHODOLOGIES. Concrete International, 25, 52-57.

Zeyad, A. (2020). Effect of fibers types on fresh properties and flexural toughness of self-compacting concrete. Journal of Materials Research and Technology, 9, 4147-4158. https://doi.org/10.1016/j.jmrt.2020.02.042.

Transportation Infrastructure Durability Center
AT THE UNIVERSITY OF MAINE

35 Flagstaff Road
Orono, Maine 04469
tidc@maine.edu
207.581.4376

www.tidc-utc.org